

A Novel Methodology to Monitor Partial Discharges in Microvoids at Solid-Solid Interfaces

Emre Kantar^{†§} and Erling Ildstad[†]

[†]Department of Electric Power Engineering, Norwegian University of Science and Technology, Trondheim, Norway

[§]Department of Electric Power Technology, SINTEF Energy Research, Trondheim, Norway

Abstract—The combination of two solid dielectrics increases the risk of partial discharge (PD) activity in microscopic cavities at the solid-solid dielectric interfaces, facilitating interface tracking failures. The main purpose of this study is to propose a novel methodology to monitor PD activities in the microvoids at solid-solid interfaces that are likely to trigger a complete interfacial failure. To scrutinize the principal mechanisms governing the interfacial breakdown, initiation, development, and propagation of discharge streamers at solid-solid interfaces were monitored using a sensitive digital camera attached to a high-voltage (HV) test setup. The captured images showed that the surface roughness and contact pressure affect the length of the vented air-filled channels at the interface. In the case of rougher surfaces, the discharged cavities formed continuous, connected discharge channels that were wider and longer than those in the case of smoother surfaces. In some cases, only microcavities were discharged and were isolated between the contact spots.

I. INTRODUCTION AND BACKGROUND

All electrical insulation systems consist of a combination of different insulating and conductive materials. The series connection of two or more dielectric materials constitutes the electrical insulation system in most high-voltage (HV) equipment and accessories. The alternating current (AC) breakdown strength (BDS) of insulation systems is limited by the lowest BDS of either the bulk insulating materials or the interface between adjacent insulating materials.

When two nominally flat, solid surfaces are brought into contact, contacts occur at discrete spots, leading to numerous cavities between adjacent contacting areas (contact spots) at the interface, as illustrated in Fig. 1.

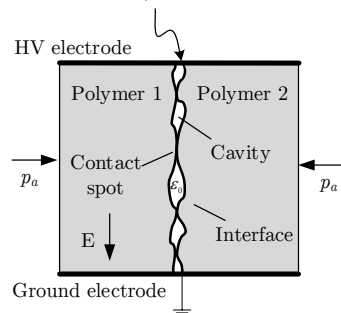


Fig. 1: Illustration of a solid-solid interface, consisting of cavities and contact spots. E is the tangential electric field, and p_a is the contact pressure.

materials and applied contact pressure (interfacial pressure) significantly affect the shape, size, and number of cavities and contact spots [1], [4]–[6]. Cavities are likely to cause

partial discharges (PD) and trigger interfacial tracking that can eventually lead to a premature electrical breakdown (BD) [4], [7]. In addition, the dielectric medium inside the cavities influences the PD inception field strength (PDIE) [8]. Once the cavities are filled with air, the electrical stress increases and its dielectric strength becomes lower than that of the surrounding bulk insulation [3], [4]. Thus, PDs are likely to be initiated in the cavities. That being the case, polymer interfaces should be scrutinized separately to explore the principal mechanisms controlling the solid-solid interface breakdown, that will eventually pave the way for the design of advanced, long-lasting, and reliable HV equipment and accessories suitable for use at higher voltages and power levels.

In the authors' previous works [8]–[12], the effects of the contact pressure, surface roughness, elastic modulus of the polymers, and insulating dielectric media surrounding the interfaces (i.e., air, water, and oil) on the longitudinal AC breakdown strength of solid-solid interfaces were examined both theoretically and experimentally. In these studies, the values of the AC BDS and PDIE of polymer interfaces were recorded, and an interface breakdown model for solid-solid interfaces was developed.

In the interface breakdown model proposed in [8], the breakdown strength of a solid-solid interface is represented by two main submodels that estimate the dielectric strength of cavities and that of contact spots individually, as illustrated in Fig. 1. In the model, the dielectric strength of cavities is predicated upon void size/shape and insulating medium filling the voids while the dielectric strength of contact spots, which restrict the propagation of discharges in the air-filled cavities/channels, is modeled using the electrical tracking resistance of the polymers in contact. The assessment of the results in this paper will be based on this theoretical model.

The results reported in [9]–[11] provide indirect implications of the interfacial PDs and breakdown activities because discharges were not directly observed; interfaces could be inspected only after the experiments. In this work, initiation, development and propagation of discharge streamers at solid-solid interfaces are intended to be observed firsthand to expand the examination of the leading mechanisms in the interfacial breakdown. The main purpose of this study is, therefore, to come up with a novel methodology that enables PD activities in the microvoids at solid-solid interfaces to be monitored, which will help clarify the leading discharge mechanisms.

II. EXPERIMENTAL PROCEDURE

Test samples and the experimental setup devised for the discharge-monitoring tests are presented in this section.

A. Type of Solid Samples

Previously performed AC breakdown and PD experiments incorporated solid-solid interfaces formed between the surfaces of two polymers that were positioned vertically on top of each other [9]–[11]. In the discharge-monitoring tests, the top sample was a smooth glass specimen very similar in dimensions to the bottom polymer sample, as shown in Fig. 2. The primary purpose of using a glass specimen is for the optical monitoring of the interface through a transparent material. Polyether ether ketone (PEEK) was used for the bottom polymer due to its high hardness that can withstand the counter pressure from the glass specimen without being deformed. PEEK is known for its high electrical integrity, excellent chemical resistance, and high mechanical properties in extreme environments and is widely used in the new dry- and wet-mate subsea connectors [8]. The relative permittivities of the PEEK and glass are 2.8 and 3.8, respectively [8].

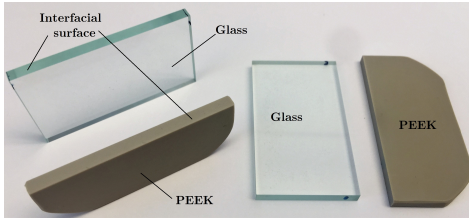


Fig. 2: Glass and PEEK samples prepared for the discharge-monitoring experiments. The interfacial surfaces of glass samples were polished by the glass workshop to achieve maximum smoothness possible.

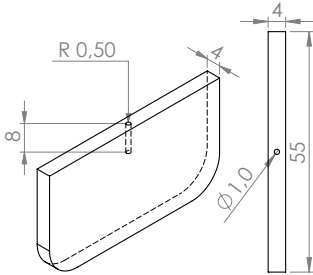


Fig. 3: PEEK sample with a cylindrical cavity of 1 mm diameter.

In [8], it is reported that the experimental challenges prompted the use of a large artificial cavity at the interface to initiate PDs at a lower voltage without inducing an interfacial breakdown immediately. A cylindrical, artificial cavity with a diameter of 1 mm, was drilled perpendicular to the electric field direction at the surface of each PEEK sample, as illustrated in Fig. 3. PDs in the artificial cavity was initiated at a significantly lower field without interfacial failure. The discharged artificial cavity generated local, intense non-homogeneous fields near its vicinity and was used to trigger PDs in the microvoids. Readers are referred to [8] for details.

The contact surfaces of the PEEK samples were polished using a table-top, grinding machine. As explained in [10], the specimens were fixed on a steel rotating disk, and a round-SiC sandpaper of the desired grit was placed on the rotating plane. The discharge experiments were performed using PEEK surfaces at two different surface roughnesses that were polished using sandpapers of grit #180 and #500.

B. Experimental Setup for Discharge-Monitoring

An illustration of the test arrangement with the dimensions of the core components is depicted in Fig. 4. The interface pressure that compresses the samples together vertically was varied using nuts and bolts while the applied force was measured by the identical load cells connected to two separate PCE Digital Force Gauges (PCE-FB 2K). A pair of Rogowski-shaped electrodes was used to apply a homogeneous electric field in the horizontal direction (x -axis w.r.t. Fig. 4). The container (no. 8) was filled with synthetic ester oil (Midel 7131) to prevent external flashovers between the electrodes.

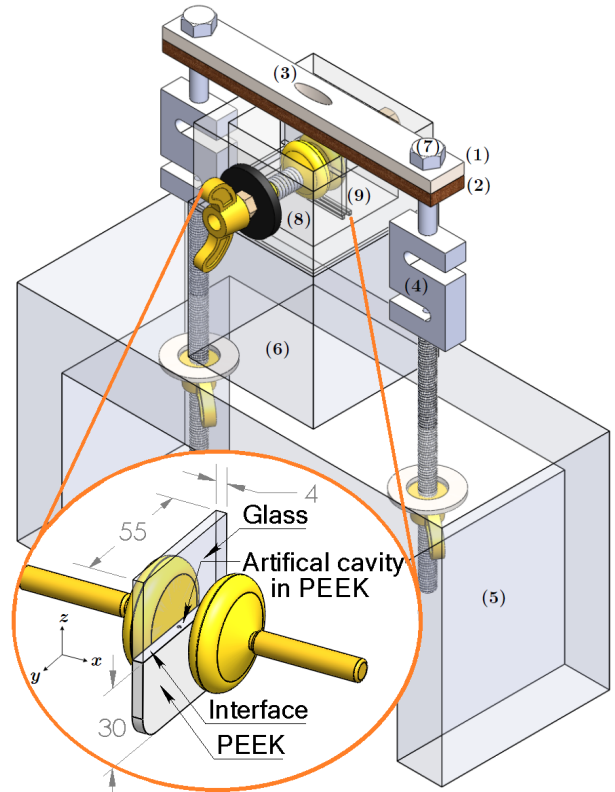


Fig. 4: Illustration of the setup used for the discharge-monitoring tests: (1) Steel metal plate used for loading. (2) Wooden plate for the cushioning between the glass and steel (identical to 1). (3) Apertures in the punched plates (1 and 2) for the camera monitoring. (4) Load cell connected to the digital force measurement gauge. (5) Main wooden base. (6) Upper support base for the glass container. (7) Bolts attached to force gauge for clamping. (8) Plexiglass container with the electrodes (40-mm diameter). (9) Solid samples: PEEK (bottom) and glass (top) of 4 mm \times 55 mm \times 30 mm. Electric field is applied in the direction of x -axis.

A charge-coupled device (CCD) camera with an image sensor from Photometrics (QuantEM 512SC) was used for capturing the light emission from the PD activities. A computer was used to control the camera via MetaMorph GUI v7.6. A long-distance microscope lens with an adjustable focus was attached to the CCD camera to monitor the interface through the openings (no. 3).

The camera and metal components were electrically grounded to protect the equipment in the unlikely case of an external flashover and to avoid floating potentials in the setup. To capture the emitted light from the discharge activity,

which is significantly dimmer than daylight, a dark-room environment was established by covering the equipment with thick black fabric.

Fig. 5 illustrates the complete test setup incorporating the CCD camera, the mechanical electrode system, and the electrical components: the variac and the transformer. Also, a coupling capacitor and an Omicron MPD 600 PD acquisition unit are connected to obtain the discharge patterns simultaneously.

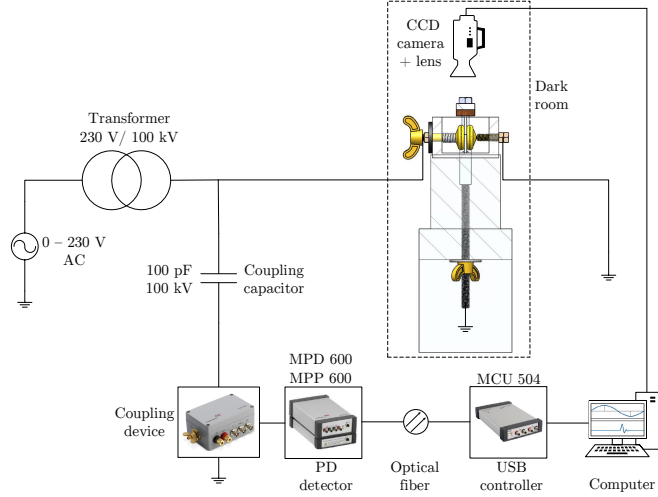


Fig. 5: Illustration of the complete test setup for the interface discharge-monitoring experiments; the voltage values are given in rms.

C. Test Procedure for Discharge-Monitoring

PEEK-glass interfaces were assembled between the electrodes at dry conditions. After the desired force was applied, the plexiglass container (no. 8) was filled with Midel 7131. Next, the optimal exposure time of the camera was adjusted in the dark environment; the setup was powered by an AC ramp voltage of 1 kV/s until PDs were initiated, and then the voltage was retained at the PD inception voltage (PDIV). The PD inception was detected by observing both the PD patterns on the GUI of Omicron MPD 600 and the discharge images from the CCD.

Pseudocolor rendering was used to distinguish between different intensities of the emitted light in the images where the red color is assigned to the most intense light emission while colder colors such as shades of blue represent reduced intensity, as depicted in Fig. 6. All of the images were captured using an exposure time of 60 s. Readers are referred to [8] for the detailed experimental procedure.

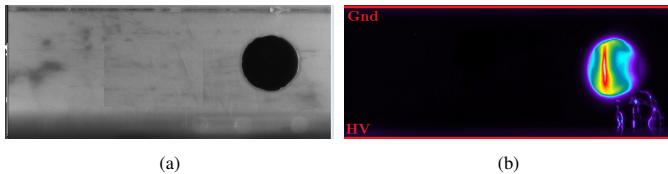


Fig. 6: Images from the CCD camera; the distance between the electrodes HV and ground (Gnd) is 4 mm: (a) Without the voltage, true-color image. (b) Discharged cavity bridging with the HV electrode, pseudocolor image.

III. RESULTS

In the experiments, interfaces between PEEK#180-glass and PEEK#500-glass were tested at contact pressures ranging between 1.16–2.5 MPa.

A. Measured PD Activity

PEEK#500-glass interfaces where PEEK samples with a 1-mm artificial cavity and without it are compared at 1.67 MPa contact pressure in Figures 7 and 8 to reveal the effect of the artificial cavity on the PD results. As seen in the phase distributions and the histograms, number of PDs is significantly higher even at considerably lower voltages in the case of PEEK with an artificial cavity. The PDIV values and the recorded charge magnitudes are also provided in Fig. 8. The most striking result to emerge from the data is that the PDIV of the PEEK with an artificial cavity is less than half of the PDIV of the PEEK without an artificial cavity.

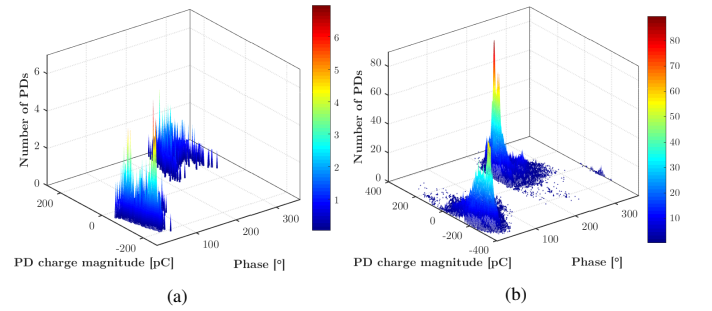


Fig. 7: Phase-charge magnitude-number of PDs plot of PEEK#500-glass at 1.67 MPa. (a) Without an artificial cavity. (b) With an artificial cavity.

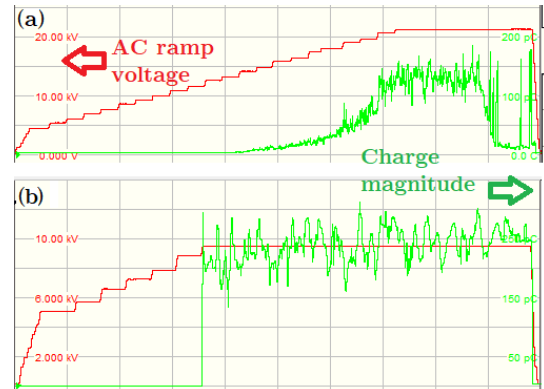


Fig. 8: Measured PDIV values of PEEK#500-glass at 1.67 MPa: (a) PEEK without an artificial cavity. (b) PEEK with an artificial cavity.

B. Monitored PD Activity

Fig. 9(a) displays the size of a microcavity in terms of pixels as compared to that of the artificial cavity with a diameter of 1 mm. Thus, the ratio of 1/15 between the pixels yields a microcavity size of 67 μm in the direction of the field. Similarly, the smallest cavity size was found to be around 36 μm considering the ratio of 5/140 in Fig. 9(b). These images indicate that sizes of the microcavities are comparable with the estimated cavity sizes (in the direction of the field) ranging between 32–137 μm , as reported in [8], [12].

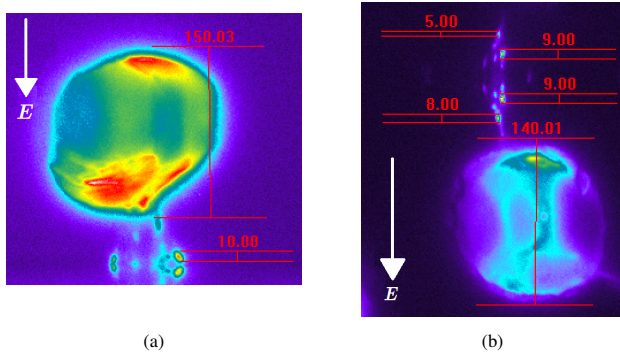


Fig. 9: Pixel size of discharged microcavities and the 1-mm artificial cavity.

Based on the discharge characteristics, the results are grouped together in Figures 10–12. The first group of images shown in Fig. 10 consists of discharged microcavities isolated from each other at the PEEK#500–glass interface. The PDs in the microcavities are likely to have been induced by the high local fields generated by the discharged artificial cavity. The discharged microcavities form a semi-conductive filament bridging the artificial cavity with one of the electrodes. The reason why it is called semi-conductive is that contact spots seem to isolate the discharged microcavities due to their non-zero interface tracking resistances [2], [8].

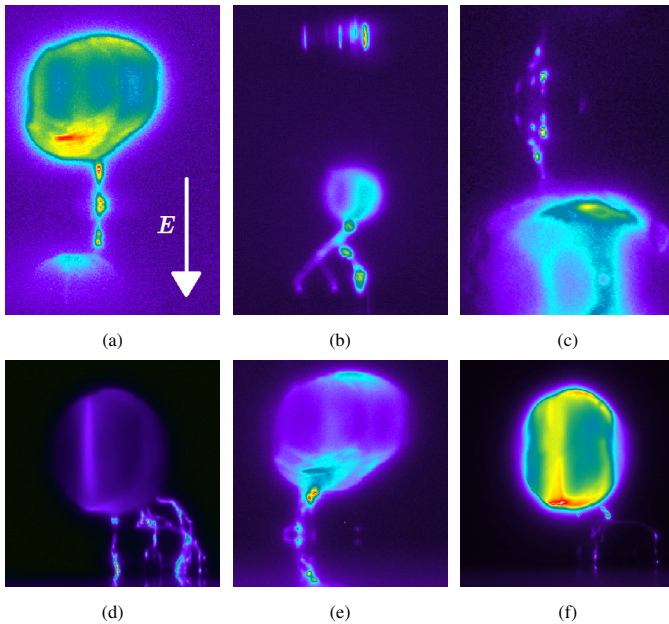


Fig. 10: Interfacial discharges induced by the 1-mm artificial cavity that were formed by isolated, discharged cavities at the PEEK#500–glass interfaces. The electric field direction shown in (a) is the same for all the images.

The next stack of images from the PEEK#500–glass interface depicts glow discharges bridging the artificial cavity with either of the electrodes based on the direction of the electric field, as displayed in Fig. 11. The continuous discharge channels suggest that streamers tend to follow vented air channels that are composed of a number of connected cavities in 3D space. Seemingly, the progressing discharge channels could not follow the shortest path to the electrodes due to

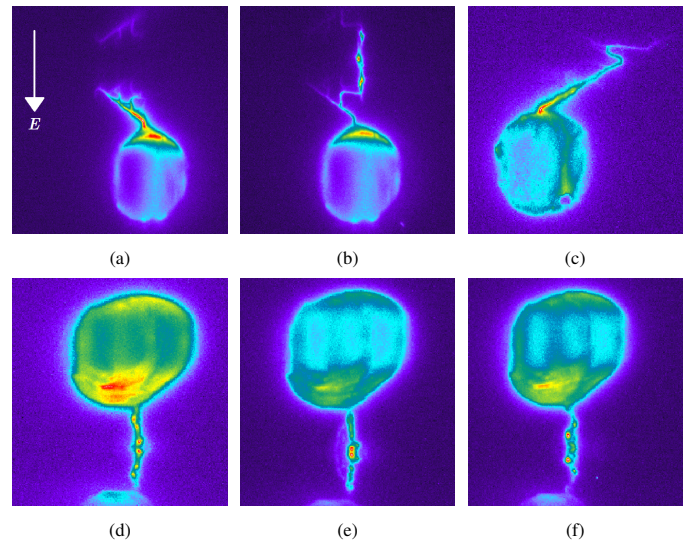


Fig. 11: Interfacial discharges induced by the 1-mm artificial cavity that were formed by continuous channels with low cross-section at the PEEK#500–glass interfaces. The field direction shown in (a) is the same for all the images.

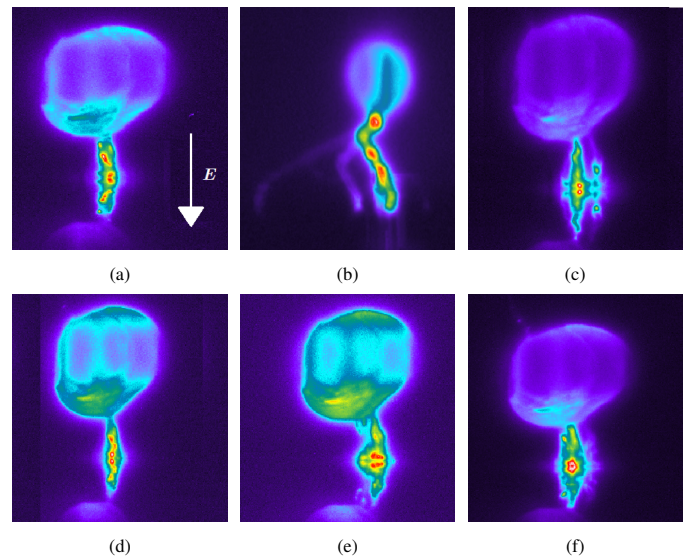


Fig. 12: Interfacial discharges induced by the 1-mm artificial cavity that were formed by continuous channels with high cross-section at the PEEK#180–glass interfaces. The field direction shown in (a) is the same for all the images.

the contact spots obstructing the discharges from directly proceeding towards the electrodes. Instead, the discharges presumably followed the air-gaps connected to each other.

Fig. 12 displays the results obtained in the case of PEEK#180–glass interfaces. As seen, the discharge channels are significantly wider (of larger cross-section) compared to those shown in Fig. 11.

IV. DISCUSSION

In Fig. 10, the cavities seem to have broken into smaller voids, resulting in fewer long air-filled channels as opposed to those shown in Figures 11 and 12. The simulated structures of the surface asperities—shown in Fig. 13 by using the data from real, measured surface profiles [8]—support the presence

of continuous vented air-gaps. Based on the difference between the simulated surfaces of PEEK#180 and PEEK#500 displayed in Fig. 13, there are larger air-gaps and fewer isolated cavities in the case of PEEK#180, likely to result in streamers with larger cross-sections, as detected in Fig. 12. Thus, the impact of the surface roughness on the width and length of the air-gaps is clearly observed that, in turn, results in stronger interfacial discharges with higher energy.

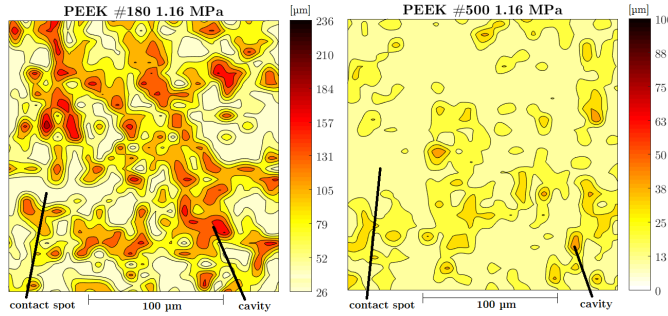


Fig. 13: Filled-contour plots of the surface asperities of the PEEK samples polished with #180 and #500 at 1.16 MPa, respectively. Color bars are in μm , where light yellow color represents the contact areas and darker colors imply cavities based on their depths [8].

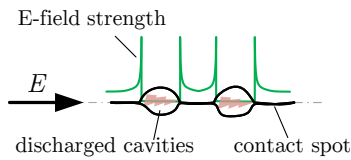


Fig. 14: An illustration of the field lines at the interface. The field is the cavities are deemed uniform [8].

contact spots. To check the likelihood of this claim, we scanned the surfaces of the samples after the discharge-monitoring experiments using a digital microscope to see if there were permanent damages at the surface such as contact spots subjected to electrical breakdown.

Fig. 15 demonstrates three microscope images of one unused and two PD-exposed PEEK samples. PD-exposed samples were subjected to the discharged artificial cavity and discharged microcavities induced by the high local fields originated from the discharged artificial cavity. As can be seen in Figures 15(b)–(c), discharges left visible traces at the surface. In addition, permanent morphological changes at the brim of the artificial cavity were detected, that are likely to have occurred due to the elevated temperatures as a result of the persistent discharges in the artificial cavity. Close to the artificial cavity, permanent damage was also spotted, as shown in Fig. 15(c) that was probably caused by the strong local PDs.

V. CONCLUSION

A novel methodology was proposed to trigger PDs in the microcavities at solid-solid interfaces without causing immediate interfacial failure. Owing to the designed experimental setup, we could obtain clear discharge images of interfacial PDs in the cases of different surface roughnesses. The results elucidated the mechanisms that give rise to the propagation of

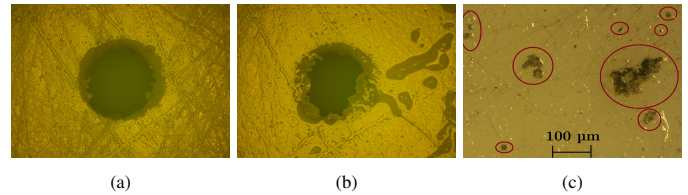


Fig. 15: PEEK surface before and after a test: (a) Before the test (unused). (b) After the test (used). (c) After the test (used), with 100X magnification.

streamers from the discharged cavities at the interface. The obtained PD activity suggested that surface roughness and contact pressure affect the number of air-filled microcavities and, in turn, the length of the vented channels composed of air-filled microcavities in 3D-space. In the case of rougher surfaces (PEEK#180–glass), the discharge channels were found to be wide and continuous whereas in the case of smoother surfaces (PEEK#500–glass), the channels were significantly thin and short. In some cases, only the microcavities were discharged and were isolated between the contact spots that indicate that the electrical tracking resistance of the contact spots has a significant role in hindering the discharge streamers from propagating.

ACKNOWLEDGMENT

This research was supported by The Research Council of Norway (no. 228344/E30) and SINTEF Energy Research. We are thankful to our colleagues Sverre Hvidsten and Frank Mauseth for their contributions.

REFERENCES

- [1] B. Zhu, Z. Jia, H. Hu, X. Ouyang, and X. Wang, “Relationship between the Interfacial DC Breakdown Voltage and the Morphology of the XLPE/SiR Interface,” *IEEE Trans. Dielectr. Electr. Insul.*, vol. 26, no. 3, Jun. 2019.
- [2] B. Zhu, Z. Jia, H. Hu, J. Xu, X. Ouyang, and X. Wang, “Interface resistivity and interfacial DC breakdown voltage of double-layer dielectrics,” *IEEE Trans. Dielectr. Electr. Insul.*, vol. 26, no. 4, pp. 1181–1189, Aug. 2019.
- [3] T. Takahashi, T. Okamoto, Y. Ohki, and K. Shibata, “Breakdown strength at the interface between epoxy resin and silicone rubber – A basic study for the development of all solid insulation,” *IEEE Trans. Dielectr. Electr. Insul.*, vol. 12, no. 4, pp. 719–724, Aug. 2005.
- [4] D. Fournier, C. Dang, and L. Paquin, “Interfacial breakdown in cable joints,” in *Proc. IEEE Int. Electr. Insul. Symp.*, 1994, pp. 450–452.
- [5] D. Fournier, “Effect of the surface roughness on interfacial breakdown between two dielectric surfaces,” in *IEEE Int. Symp. Electr. Insul.*, vol. 2, IEEE, 1996, pp. 699–702.
- [6] B. Du, X. Zhu, L. Gu, and H. Liu, “Effect of surface smoothness on tracking mechanism in XLPE-Si-rubber interfaces,” *IEEE Trans. Dielectr. Electr. Insul.*, vol. 18, no. 1, pp. 176–181, 2011.
- [7] F. H. Kreuger, *Partial discharge detection in high-voltage equipment*. Butterworths London, 1989.
- [8] E. Kantar, “Longitudinal AC Electrical Breakdown Strength of Polymer Interfaces,” Ph.D. dissertation, Norwegian Uni. Sci. Tech., 2019.
- [9] E. Kantar, D. Panagiotopoulos, and E. Ildstad, “Factors Influencing the Tangential AC Breakdown Strength of Solid-Solid Interfaces,” *IEEE Trans. Dielectr. Electr. Insul.*, vol. 23, no. 3, pp. 1778–1788, 2016.
- [10] E. Kantar, S. Hvidsten, F. Mauseth, and E. Ildstad, “Longitudinal AC Breakdown Voltage of XLPE-XLPE Interfaces Considering Surface Roughness and Pressure,” *IEEE Trans. Dielectr. Electr. Insul.*, vol. 24, no. 5, pp. 3047–3054, 2017.
- [11] E. Kantar, S. Hvidsten, and E. Ildstad, “Effect of Material Elasticity on the Longitudinal AC Breakdown Strength of Solid-Solid Interfaces,” *IEEE Trans. Dielectr. Electr. Insul.*, vol. 26, no. 2, pp. 655–663, 2019.
- [12] E. Kantar, S. Hvidsten, F. Mauseth, and E. Ildstad, “A Stochastic Model for Contact Surfaces at Polymer Interfaces Subjected to an Electrical Field,” *Tribology Int.*, vol. 127, pp. 361–371, 2018.